

Recent Results from the L3 Experiment ¹

Salvatore Mele²

EP Division, CERN, CH1211, Genève 23, Switzerland

On behalf of the L3 Collaboration

Abstract

A data sample corresponding to an integrated luminosity of 232 pb^{-1} was collected in 1997 and 1998 by the L3 experiment at LEP in e^+e^- collisions at centre-of-mass energies between 181.7 GeV and 188.7 GeV. Pair production of fermions and bosons is studied and compared with the Standard Model expectations. Events with a single detected photon or W boson are also considered. The measurement of several Standard Model cross sections is discussed. The presence and the magnitude of triple couplings of charged and neutral electroweak gauge bosons is investigated. These processes are used to probe New Physics beyond the Standard Model, including the existence of extra spatial dimensions.

1 Introduction

The L3 detector [1] started in 1989 to collect data at LEP in e^+e^- collisions at a centre-of-mass energy $\sqrt{s} \simeq m_Z$. It has contributed to the success of the LEP I programme, when more than twenty millions of Z bosons were produced testing the Standard Model of electroweak interactions [2] (SM) with an impressive precision [3]. In 1995 the campaign for the gradual increase of the LEP beam energy started, bringing the experiments in the so called LEP II era. In the present paper I will give a snapshot of several L3 results from the high integrated luminosity runs of 1997 and 1998 at an average \sqrt{s} of 182.7 GeV and 188.7 GeV, respectively. These two energies will be indicated as 183 GeV and 189 GeV hereafter and correspond to 55 pb^{-1} and 176 pb^{-1} of integrated luminosity, respectively. Some of the results described here are published, others are preliminary. Results from the lower energy runs at 133 – 140 GeV with 10 pb^{-1} of integrated luminosity and 161 GeV – 172 GeV with 21 pb^{-1} , are sometimes included in the discussed analyses.

These results, which are only a subsample of the LEP II physics program carried out by the L3 experiment, are classified in the following according to the type and number of particles primarily produced in the e^+e^- interactions: two fermions, two W, just one W, two or more photons, one Z and a photon and two Z. Tests of theories of gravity with extra spatial dimensions are finally presented.

2 Two fermions

Fermion pair production is a fundamental process to be studied at LEP II both as a verification of SM predictions and as a necessary check of the understanding of the detector performance. A kinematically favoured configuration in fermion pair production at energies above the Z pole is the emission of a hard initial state photon which lowers the effective centre-of-mass energy, $\sqrt{s'}$, to the Z resonance. This process is known as “radiative return to the Z” and yields high energy photons either in the detector or almost collinear with the beams and hence undetected.

It is customary to express the results of the cross sections and forward-backward asymmetries of the fermions by separating the full data sample ($\sqrt{s'}/s > 0.1$) and the purely high energy one, from which the radiative return to the Z events are rejected ($\sqrt{s'}/s > 0.85$). Table 1 reports the L3 results for the two considered energies [4] for quark, muon, tau and electron pairs. A good agreement with the SM predictions is observed. Figure 1 presents the evolution with \sqrt{s} of the fermion pair cross section as predicted by the SM and measured by the L3 experiment.

From the analysis of events with a single photon visible in the detector [5] it is possible to derive the radiative neutrino pair production cross section. At 189 GeV the measured cross section is:

$$\sigma_{e^+e^- \rightarrow \nu\bar{\nu}\gamma(\gamma)}(189 \text{ GeV}) = 5.25 \pm 0.22 \pm 0.07 \text{ pb},$$

¹Invited talk at the XIV International Workshop on Quantum Field Theories and High Energy Physics, QFTHEP99, Moscow, Russia, 27 May – 2 June, 1999, to appear in the proceedings.

² On leave of absence from INFN-Sezione di Napoli, Italy. E-mail: Salvatore.Mele@cern.ch

where the first error is statistical and the second systematic. The extrapolation of this value to the total cross section reads:

$$\sigma_{e^+e^- \rightarrow \nu\bar{\nu}(\gamma)}(189 \text{ GeV}) = 58.3 \pm 2.5 \text{ pb.}$$

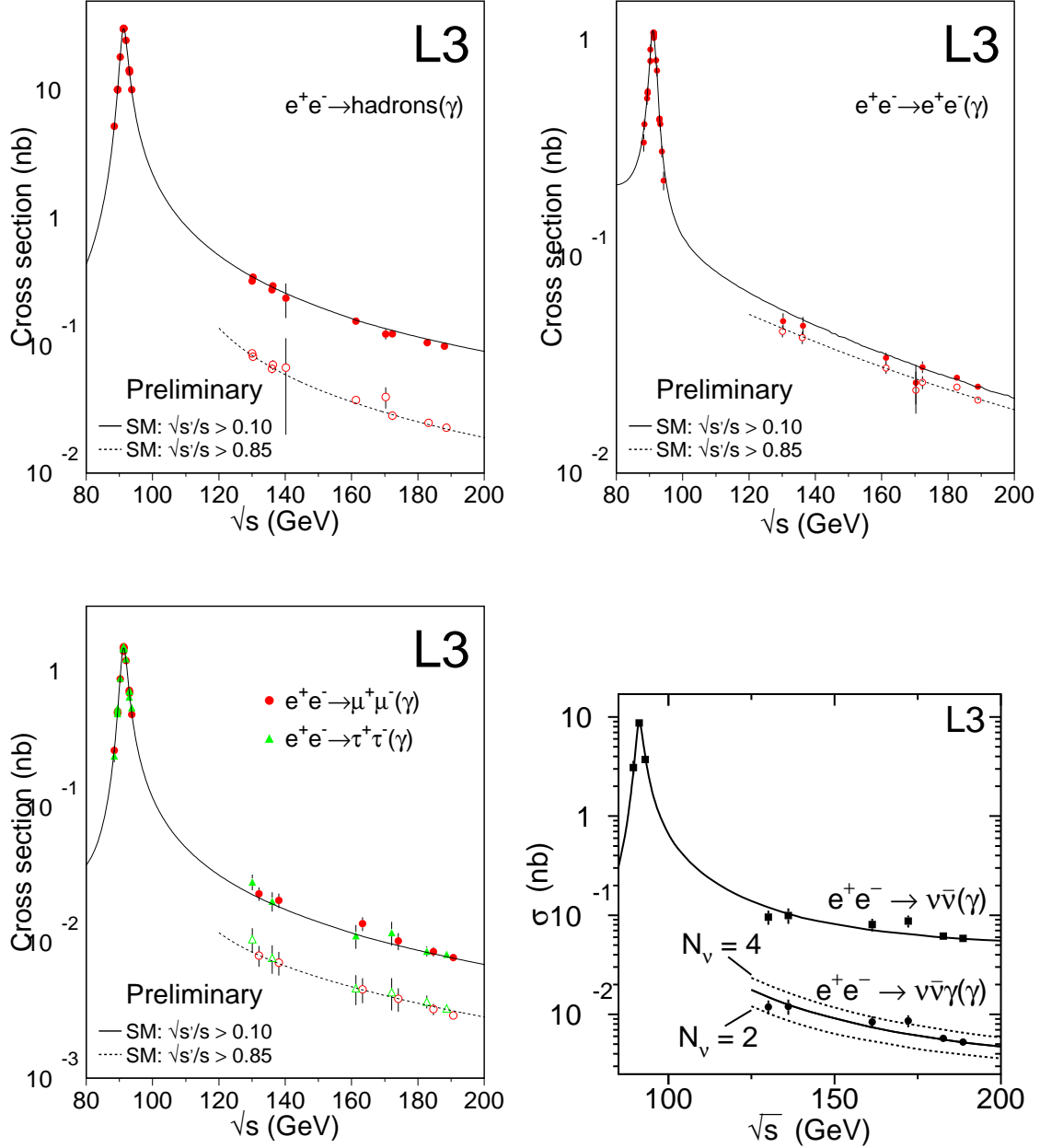


Figure 1: Fermion pair cross section evolution as a function of the centre-of-mass energy.

Figure 1 shows the evolution of these two cross sections as a function of \sqrt{s} as well as a comparison of $\sigma_{e^+e^- \rightarrow \nu\bar{\nu}\gamma(\gamma)}$ with the SM expectations in presence of 2, 3 or 4 neutrino species. From the photon energy spectrum it is possible to determine the number N_ν of light neutrino species as $N_\nu = 3.05 \pm 0.11 \pm 0.04$, with respectively statistic and systematic errors. The average of this result with L3 results at the Z pole [6] yields:

$$N_\nu = 3.011 \pm 0.077.$$

Channel	Cross sections (pb)		Asymmetries	
	$\sqrt{s'/s} > 0.1$	$\sqrt{s'/s} > 0.85$	$\sqrt{s'/s} > 0.1$	$\sqrt{s'/s} > 0.85$
$\sqrt{s} = 183 \text{ GeV}$				
$e^+e^- \rightarrow q\bar{q}(\gamma)$	105.9 ± 1.5	24.2 ± 0.8	–	–
$e^+e^- \rightarrow \mu^+\mu^-(\gamma)$	8.6 ± 0.7	3.2 ± 0.3	0.38 ± 0.07	0.56 ± 0.07
$e^+e^- \rightarrow \tau^+\tau^-(\gamma)$	8.6 ± 0.8	3.7 ± 0.4	0.28 ± 0.09	0.59 ± 0.09
$e^+e^- \rightarrow e^+e^-(\gamma)$	27.5 ± 0.7	24.9 ± 0.7	0.80 ± 0.02	0.83 ± 0.02
$\sqrt{s} = 189 \text{ GeV}$				
$e^+e^- \rightarrow q\bar{q}(\gamma)$	99.4 ± 0.8	22.8 ± 0.4	–	–
$e^+e^- \rightarrow \mu^+\mu^-(\gamma)$	7.7 ± 0.3	3.4 ± 0.2	0.26 ± 0.03	0.57 ± 0.04
$e^+e^- \rightarrow \tau^+\tau^-(\gamma)$	8.0 ± 0.4	3.1 ± 0.2	0.29 ± 0.03	0.53 ± 0.05
$e^+e^- \rightarrow e^+e^-(\gamma)$	25.1 ± 0.4	21.7 ± 0.4	0.82 ± 0.01	0.85 ± 0.01

Table 1: Experimental cross sections and asymmetries of fermion pair production.

The study of fermion pairs constitutes also an interesting probe of possible New Physics beyond the SM. The examples of Supersymmetry and contact interactions will be highlighted in the following.

The Minimal Supersymmetric Standard Model [7] (MSSM) introduces a new quantum number, the R-parity [8]. This quantity distinguishes ordinary particles and supersymmetric ones, requiring an even number of the latter in each interaction vertex and hence constraining the lightest supersymmetric particle to be stable. As a consequence of the negative results of the search for supersymmetric particles at the present colliders, it is interesting to investigate possible signatures of supersymmetric models with broken R-parity [9], where triple vertices with a supersymmetric particle and two SM ones are allowed. Some of these signatures are the production of a pair of electrons in e^+e^- collisions mediated by the s - or t -channel muon or tau sneutrino exchange, the production of a muon pair via the s -channel exchange of a tau sneutrino or that of a tau pair via a muon sneutrino. These sneutrinos are the scalar partner of the SM neutrinos. The presence of these processes would lead to a resonant structure in the lepton pair production cross section around the mass of the exchanged sneutrino. From the investigation [10] of the cross sections and asymmetries of final states electrons, muons and tau, no evidence for such signatures is found and limits at 95% confidence level (CL) are derived on the coupling constant of the sneutrino as a function of its mass, as reported in Figure 2, for the electron and muon signatures.

Contact interactions can be thought of as a general formalism to describe New Physics from a scale much higher than the energy of an investigated process. An example is the contact interaction structure used by Fermi to describe the beta decay [11] fifty years before colliders reached the necessary energy to produce the W boson, whose mass is now known to be the scale of the process. Analogously a new interaction of coupling constant g and scale Λ yet far above direct experimental reach can be probed in fermion pair production in e^+e^- interactions. It is sketched in Figure 3 and is parametrised via an effective Lagrangian [12]:

$$\mathcal{L} = \frac{1}{1 + \delta_{ef}} \sum_{i,j=L,R} \eta_{ij} \frac{g^2}{\Lambda_{ij}^2} (\bar{e}_i \gamma^\mu e_i) (\bar{f}_j \gamma_\mu f_j),$$

where e_i and f_j are the left- and right-handed initial state electron and final state fermion fields and the coefficients $\eta_{ij} = 0, \pm 1$ allow to choose which helicities contribute to the fermion pair production within the different models, as listed in Table 2.

The contact interaction will manifest itself in the differential cross sections of a given phase space parameter as a function of $1/\Lambda^2$ in the interference terms of SM and New Physics and as a function of $1/\Lambda^4$ for the pure New Physics part. The search for contact interactions [13] proceeds by performing a χ^2 fit to the charged fermion pair cross sections and asymmetries measurements presented above, with Λ as a free parameter with the convention $g^2/4\pi = 1$. The results of those fits are compatible with the SM for all the possible choices of the helicities and 95% CL limits as high as 12 TeV are set on the scale Λ of some models. All the limits are presented in Figure 3, where Λ_+ and Λ_- denote respectively the

limits in the case of the upper and lower signs of the η_{ij} parameters of Table 2. Lower energy data [14] are also included.

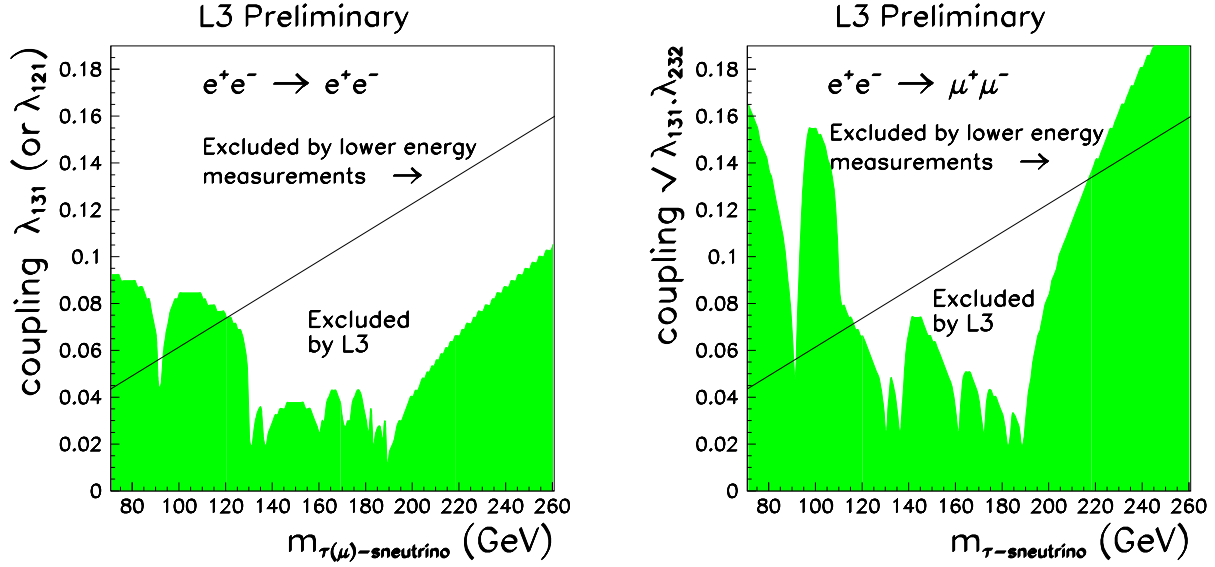


Figure 2: Limits at 95% CL on the R parity violating coupling as a function of the mass of the exchanged sneutrino.

Model	LL	RR	LR	RL	VV	AA	LL+RR	LR+RL	LL-RR
η_{LL}	± 1	0	0	0	± 1	± 1	± 1	0	± 1
η_{RR}	0	± 1	0	0	± 1	± 1	± 1	0	± 1
η_{LR}	0	0	± 1	0	± 1	± 1	0	± 1	0
η_{RL}	0	0	0	± 1	± 1	± 1	0	± 1	0

Table 2: Helicities contributions in different models of contact interactions.

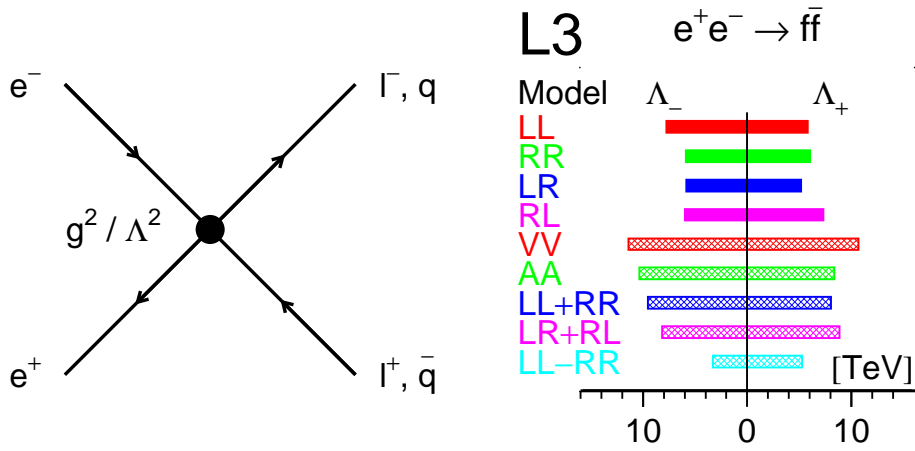


Figure 3: Feynman diagram for the contact interactions and 95% CL limits on their scale in different models.

3 Two W

The study of W pair production constitutes the core of the LEP II physics program and started in 1996 when the centre-of-mass energy of the LEP machine reached the threshold of 161 GeV. The SM describes this process at the lowest order with three diagrams: the t -channel neutrino exchange and the s -channel exchange of a Z or a photon. These last two diagrams are of crucial importance in the SM as they are a manifestation of its non Abelian structure that allows the triple vertices, ZWW and γ WW, of electroweak gauge bosons.

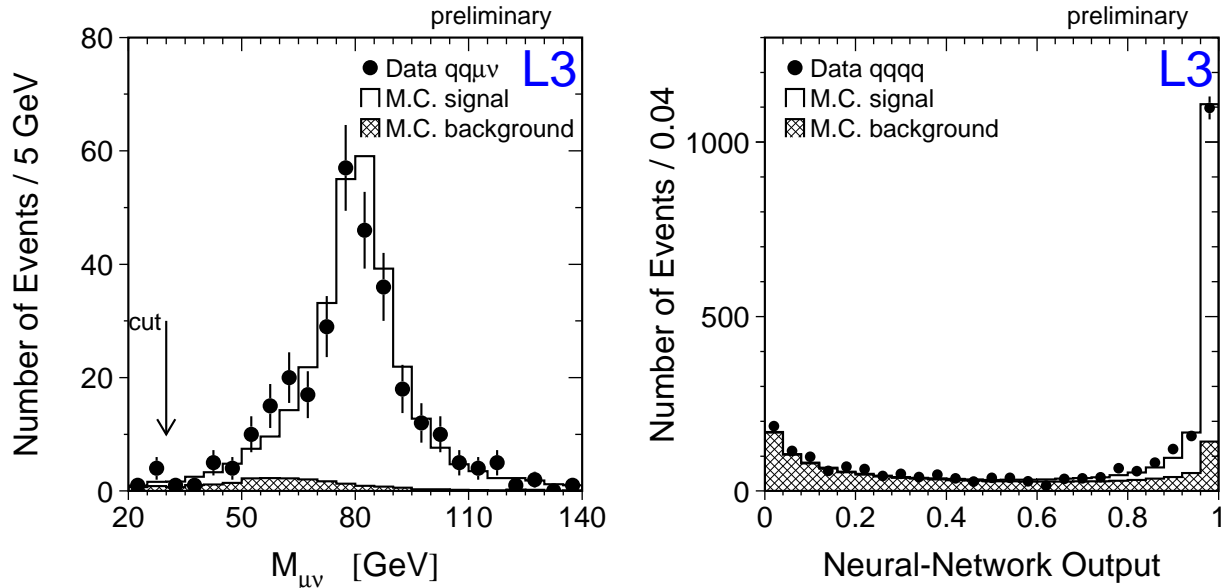


Figure 4: Selection variables for W pair events.

Detailed descriptions of the combined results of the four LEP experiments are presented elsewhere [15]. In the following, emphasis will be put on results achieved by the L3 experiment. All these results start from a selection of W pair events in the collected data sample. Five selections are devised to cope with the fully leptonic decay of the W pair, its semileptonic decay in a quark pair and an electron, a muon or a tau together with their associated neutrinos and finally its fully hadronic decay. Examples of selection variables are reported in Figure 4 for semileptonic decays of the W pair into a muon and its neutrino and fully hadronic decays. The latter is selected by means of a neural network. A high purity is achieved and combining all the decay modes, correcting for the contributions to the same final states from diagrams other than the W pair production, the cross section of W pair production is measured as [16]:

$$\sigma_{e^+e^- \rightarrow WW}(189 \text{ GeV}) = 16.25 \pm 0.38 \pm 0.27 \text{ pb},$$

where the first error is statistical and the second systematic.

Figure 5 presents the evolution of the WW cross section with \sqrt{s} as measured by L3, compared with the theory predictions. Predictions for W pair production via only the electron neutrino t -channel exchange are also reported together with those in absence of the triple gauge boson vertex ZWW. The evidence of the presence of the γ WW and ZWW constitutes an impressive proof of the non Abelian structure of the SM. The measured cross sections are in good agreement with the SM prediction even though this comparison is limited by the theory uncertainty, as large as 2%, due to be reduced to about 0.5% in the near future [17].

The two vertices γ WW and ZWW are described by means of seven complex coupling each [18]. At energies below the scale of possible New Physics, only the real part of the couplings is of interest.

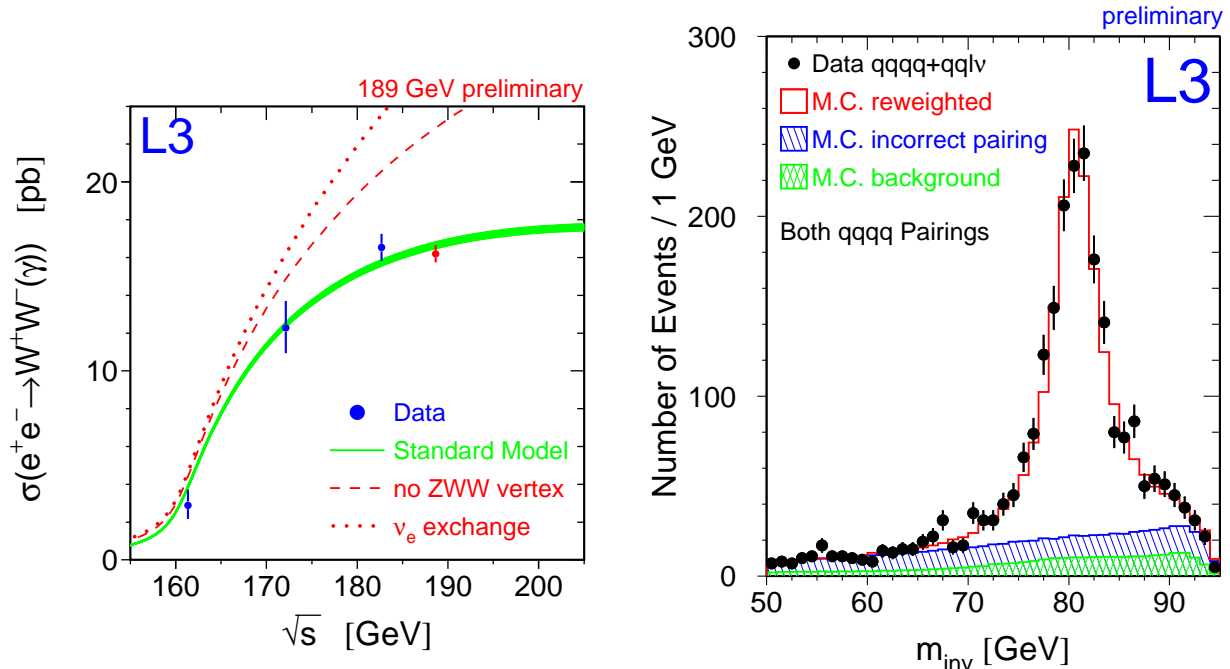


Figure 5: Evolution with the centre-of-mass energy of the W pair production cross section and distribution of the reconstructed W mass used in the fit.

The simultaneous determination of these parameters is impossible with the available statistics and their number is then restricted to five by first discarding the C-, P- and CP-violating ones and assuming electromagnetic gauge invariance. The extra requirement of custodial SU(2) symmetry allows to further reduce the number of independent couplings to just three: g_1^Z , κ_γ and λ_γ . It is interesting to relate these three couplings to basic physical quantities. g_1^Z is the weak coupling strength of the produced W pair to the exchanged Z boson, while κ_γ and λ_γ enter in the definition of the static magnetic dipole μ_W and electric quadrupole Q_W momenta of the W boson:

$$\mu_W = \frac{e}{2m_W}(1 + \kappa_\gamma + \lambda_\gamma); \quad Q_W = \frac{e}{2m_W}(1 + \kappa_\gamma - \lambda_\gamma).$$

Apart from the total cross section measurement, more information on these couplings is provided by the distribution of the polar angle of the produced W bosons and their fermion decay angles. From an analysis of hadronic and semileptonic decays of the W pair the values of these couplings are measured as [19]:

$$g_1^Z = 0.98 \pm 0.07 \pm 0.03; \quad \kappa_\gamma = 0.88_{-0.12}^{+0.14} \pm 0.08; \quad \lambda_\gamma = 0.00 \pm 0.07 \pm 0.03,$$

where the first error is statistical and the second systematic. These values are in perfect agreement with the expected SM values of 1, 1 and 0, respectively. This agreement is also found if two- or three-parameter fits are performed.

The selected events in each of the semileptonic and hadronic decay modes of the W pairs are used separately to determine the mass and the width of the W boson. Kinematic constraints are applied on the events and the weighted average mass M_{inv} is constructed for each of them. The value of this mass in data is compared to reweighted Monte Carlo (MC) events with a complex fit algorithm [20] to measure the W mass. Figure 5 presents the distribution of M_{inv} for data collected at 189 GeV and the fit MC. The average of the result of the fit procedure to all the W pair decay channels at 172 GeV [21], 183 GeV [22] and 189 GeV, including the mass measurement from the threshold production cross section at 161 GeV [23] and 172 GeV [24] is:

$$M_W = 80.43 \pm 0.11 \text{ GeV},$$

in agreement with the SM expectation observed from a combined fit to the available data [3]. If the W width is left free in these fits, its value is measured in the previous data sample as:

$$\Gamma_W = 2.12 \pm 0.25 \text{ GeV}.$$

4 Just one W

In the fall of 1996 LEP was running at $\sqrt{s} = 172 \text{ GeV}$ and an unexpected number of acoplanar hadronic event with large missing energy was observed by the L3 analyses surveying the data for New Physics signatures. Contrarily to our hopes these events had a poor content of b quarks, and hence were incompatible with the hypothesis of an Higgs boson produced in association to a Z decaying into neutrinos. The first single W events were observed, as expected [25]. This was confirmed by counting events with a nothing but a single lepton in the detector to be in the relative amount with respect to the number of hadronic events as expected from the W branching ratios [26].

Even though a discovery was missed, sound physics information is extracted from this kind of events. The so called single W signal is a subset of the 20 diagrams that lead to the production of four fermions in the final state, two of which come from the decay of a W, the other two being an electron and its neutrino. The collective name of CC20 indicates this $e^+e^- \rightarrow e^+\nu_e f\bar{f}'$ process and its charge conjugate. In the case of interest, the process occurs via the t -channel exchange of a virtual W from the incoming electron or positron and a virtual photon from the other incoming particle, giving a real W via a $WW\gamma$ vertex. The cross section for single W production is strongly peaked for almost unscattered electrons or positrons and presents several challenges in its calculation [17]. This behaviour requires the introduction of some phase space cuts for the definition of the signal:

$$|\cos\theta_{e^+}| > 0.997; \quad \min(E_f, E_{f'}) > 15 \text{ GeV}; \quad |\cos\theta_{e^-}| > 0.75 \quad (\text{for } e^+\nu_e e^-\bar{\nu}_e).$$

The angles refer to the polar angles with respect to the beam line and charge conjugate particles are also included. E_f and $E_{f'}$ are the energies of the fermions. The application of this signal definition to the CC20 processes yields a single W sample with a purity of 90%.

The presence of only the $WW\gamma$ vertex makes this process suitable for an accurate study of the electromagnetic couplings of the W boson, namely its static magnetic dipole μ_W and electric quadrupole Q_W , introduced above.

The increasing cross section and the high integrated luminosities collected at the two energies under investigation allow a good improvement in the determination of the single W cross section [27]. Hadronic decays of the single W are separated from the background events by means of their kinematic characteristics combined into a neural network. The single lepton signature is exploited to remove background events and the distribution of its energy is retained as a final discriminating variable. A binned maximum likelihood fit to these two variables allows to determine the cross sections for single W production as:

$$\sigma_{e^+e^- \rightarrow e\nu_e W}(189 \text{ GeV}) = 0.53_{-0.11}^{+0.12} \pm 0.03 \text{ pb},$$

where the first error is statistical and the second systematic. Figure 6 compares this cross section and the lower energy ones to the SM predictions obtained with the EXCALIBUR [28] and GRC4F [29] MC programs. The experimental precision approaches the theoretical one.

With a binned maximum likelihood fit similar to the one used for the cross section determination, it is possible to measure the electromagnetic coupling of the W boson as:

$$\kappa_\gamma = 0.93_{-0.17}^{+0.15}; \quad \lambda_\gamma = -0.30_{-0.19}^{+0.68}.$$

The precision of κ_γ is comparable to that of the conventional investigation through W pair production. It should be noted that these measurements come from a two-dimensional fit, whose contours are also presented in Figure 6.

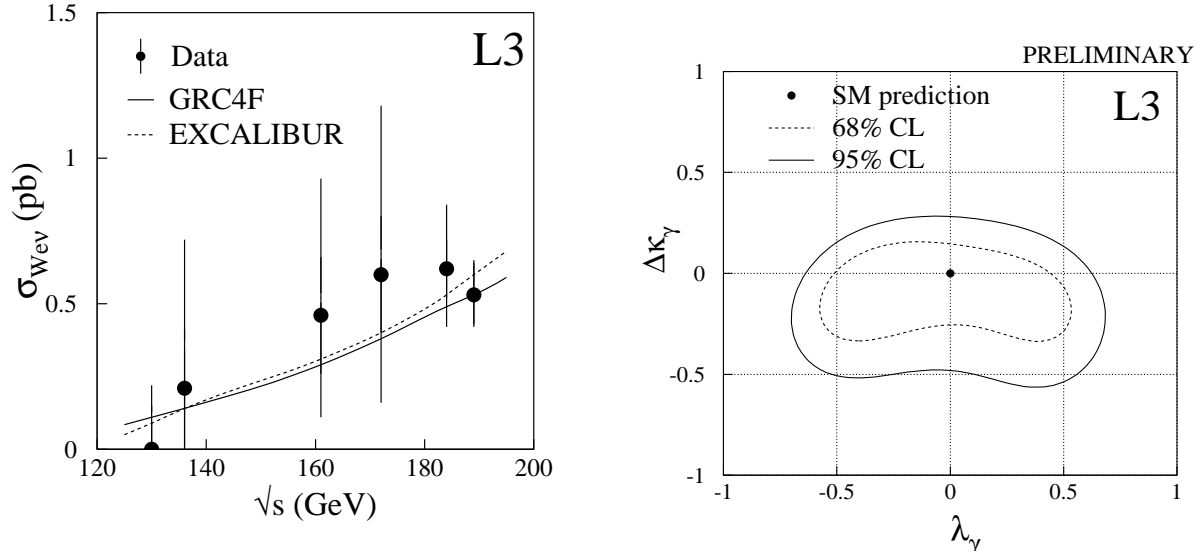


Figure 6: Evolution of the single W cross section with the centre-of-mass energy and determination of the W electromagnetic couplings. $\Delta\kappa_\gamma$ stands for the deviation of κ_γ from the SM value of 1.

5 Two (or more) photons

Multiphoton production in e^+e^- interactions is dominated by QED also at these high energies. This process has a clean experimental signature in the high-performance L3 electromagnetic calorimeter with a negligible background. The sensitivity of this process to deviations from QED increases with \sqrt{s} , making it well suitable to probe New Physics beyond the SM.

The number of observed and expected events with two or more photons in the polar angular range $16^\circ < \theta_\gamma < 164^\circ$ and with energies above 1 GeV is reported in Table 3 for the two energies under study [30]; perfect agreement is observed with the SM predictions. From these events the cross sections in the fiducial volume are extracted as:

$$\sigma_{e^+e^- \rightarrow \gamma\gamma(\gamma)}(183 \text{ GeV}) = 12.2 \pm 0.6 \text{ pb}$$

$$\sigma_{e^+e^- \rightarrow \gamma\gamma(\gamma)}(189 \text{ GeV}) = 11.6 \pm 0.3 \text{ pb}$$

	$\sqrt{s} = 183 \text{ GeV}$		$\sqrt{s} = 189 \text{ GeV}$	
	Observed	Expected	Observed	Expected
2γ	436	453	1302	1345
3γ	23	24	72	69
4γ	1	0	0	0

Table 3: Number of observed and expected multi-photon events at 183 GeV and 189 GeV.

These cross sections are compared in Figure 7a with the QED prediction as a function of \sqrt{s} . Lower energy data [31] are also presented together with the event display of a selected four visible photon event. An extra low energy photon is present in the detector. The kinematics is compatible with a fifth photon escaping down the uninstrumented beam line.

Deviations from QED are expressed in terms of effective Lagrangians and affect the expected differential cross section $d\sigma^{\text{QED}}/d\Omega$ by means of an extra multiplicative term with a different angular structure.

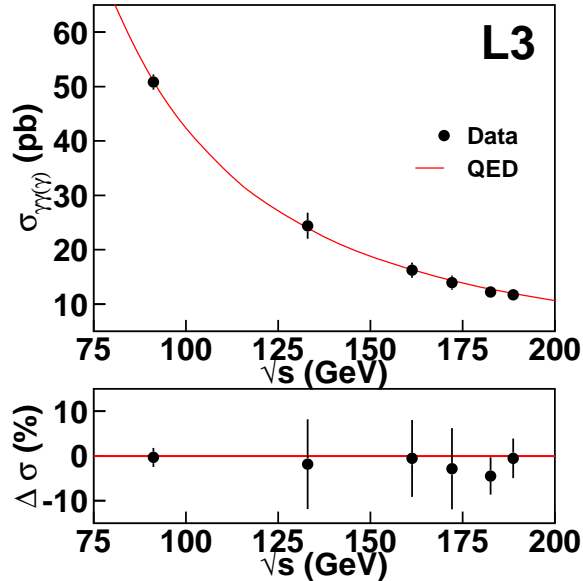


Figure 7: Evolution of the multiple hard photon production cross section with the centre-of-mass energy and side view event display of the highest multiplicity selected event. Four photons are identified, a fifth escapes along the beam pipe and a possible sixth photon is detected with energy below the identification threshold set to 1 GeV by this analysis.

Two general forms are considered [32]:

$$\frac{d\sigma}{d\Omega} = \frac{d\sigma^{\text{QED}}}{d\Omega} \left(1 + \frac{s^2}{\alpha \Lambda^4} (1 - \cos^2 \theta_\gamma) \right)$$

$$\frac{d\sigma}{d\Omega} = \frac{d\sigma^{\text{QED}}}{d\Omega} \left(1 + \frac{s^3}{32\pi\alpha^2 \Lambda'^6} \frac{1 - \cos^2 \theta_\gamma}{1 + \cos^2 \theta_\gamma} \right),$$

where α is the electromagnetic coupling and the parameters Λ and Λ' have the dimension of an energy. Alternatively the so called cut-off parameters Λ_\pm are also considered. They are linked to Λ by the relation $\Lambda^4 = \pm(2/\alpha)\Lambda_\pm^4$. A simultaneous fit to the differential distribution of the selected events at the considered energies and below does not present any deviation from the SM and the following 95% CL limits are extracted on these deviations from QED:

$$\Lambda > 1304 \text{ GeV}; \quad \Lambda_+ > 320 \text{ GeV}; \quad \Lambda_- > 282 \text{ GeV}; \quad \Lambda' > 702 \text{ GeV}.$$

Photon pairs can be also produced via the t -channel exchange of an excited electron. This interaction is described by a phenomenological Lagrangian [33] with the scale of the interaction as a free parameter. Identifying it with the mass of the excited electron, m_{e^*} , limits at 95% CL are set as:

$$m_{e^*} > 323 \text{ GeV (non-chiral)} \quad m_{e^*} > 282 \text{ GeV (chiral)},$$

according to the chirality of the interaction.

6 One photon and one Z

The non Abelian structure of the SM predicts the existence at tree level of the triple vertex of one neutral and two charged bosons, γWW and ZWW , whose presence is successfully verified at LEP, as

already reported above. The triple vertices of neutral bosons, $\gamma\gamma Z$, γZZ , and ZZZ are on the other hand forbidden at tree level in the SM. The possible presence of the first two of them, is probed by the associated production of a Z boson and a photon in e^+e^- collision. In the SM this process takes place via the t -channel electron exchange, that is nothing else than the radiative return to the Z process described above, yielding almost monoenergetic photons. The SM cross section of this process decreases with \sqrt{s} while the possible anomalous contribution coming from a t -channel Z or photon exchange does not, making the study of this process of interest with the increase of the LEP beam energy.

The $Z\gamma V$ vertex, with V either a photon or a Z, is parametrised as [18, 34]:

$$\Gamma_{Z\gamma V}^{\alpha\beta\mu}(q_1, q_2, P) = i \frac{s - m_V^2}{m_Z^2} \times \left\{ h_1^V (q_2^\mu g^{\alpha\beta} - q_2^\alpha g^{\mu\beta}) + \frac{h_2^V}{m_Z^2} P^\alpha (P \cdot q_2 g^{\mu\beta} - q_2^\mu P^\beta) + h_3^V \epsilon^{\mu\alpha\beta\rho} q_{2\rho} - \frac{h_4^V}{m_Z^2} P^\alpha \epsilon^{\mu\beta\rho\sigma} P_\rho q_{2\sigma} \right\},$$

where q_1 , q_2 and P are the four-momenta of the Z, γ and V bosons. Eight couplings appear in the above expression, four for each V boson. As in the W case, only the real part of these couplings are of interest in absence of indications for New Physics. The couplings h_1^V and h_2^V are zero in the SM at tree level and violate the CP symmetry while h_3^V and h_4^V preserve it and have an estimated value of 10^{-4} from higher order SM processes. The effect of a value of these couplings different from zero would manifest itself as an enhancement of the number of $Z\gamma$ events, more pronounced for photons emitted at a large polar angle.

The experimental selection of $Z\gamma$ events [35] proceeds in the highest branching ratio channels $q\bar{q}\gamma$ and $\nu\bar{\nu}\gamma$. A good agreement is found between the number of selected events and the SM expectations.

Five variables describe the phase space of the $ff\gamma$ events, the energy and the two angles of the photon and the two angles of one of the fermions in the Z reference frame. An unbinned maximum likelihood fit is performed in this five dimensional space for each of the eight couplings, fixing the other seven to zero. All the measured values are consistent with the SM and 95% CL limits are extracted as:

$$\begin{aligned} -0.16 \leq h_1^Z \leq 0.09; \quad -0.07 \leq h_2^Z \leq 0.11; \quad -0.22 \leq h_3^Z \leq 0.10; \quad -0.06 \leq h_4^Z \leq 0.14; \\ -0.12 \leq h_1^\gamma \leq 0.09; \quad -0.06 \leq h_2^\gamma \leq 0.07; \quad -0.12 \leq h_3^\gamma \leq 0.01; \quad -0.01 \leq h_4^\gamma \leq 0.09. \end{aligned}$$

Figure 8 presents the 95% CL contours if a two-parameter fit is performed on the pairs of couplings with the same CP-parity and involving the exchange of the same neutral boson.

7 Two Z

The data set under investigation was collected above the production threshold of Z boson pairs. This process is of particular interest as it constitutes an irreducible background for the search of the SM Higgs boson and to several other processes predicted by theories beyond the SM. In addition it allows the investigation of possible triple neutral gauge boson couplings, ZZZ and $ZZ\gamma$, forbidden by the SM.

The experimental investigation of ZZ production [36, 37] is made difficult by its rather low cross section, compared with competing processes that constitute large and sometimes irreducible backgrounds.

The Z pair signal is defined starting from generator level phase-space cuts on four fermion final states: the invariant mass of both generated fermion pairs must be between 70 GeV and 105 GeV. This criterion has to be satisfied by at least one of the two possible pairings of four same flavour fermions. In the case in which fermion pairs can originate from a charged-current process the masses of the fermion pairs susceptible to come from W decays are required to be either below 75 GeV or above 85 GeV. Events with electrons in the final state are rejected if $|\cos\theta_e| > 0.95$, where θ_e is the electron polar angle.

The expected cross sections for the different final states are computed with EXCALIBUR MC and amount to a total of 0.25 pb at 183 GeV and 0.66 pb at 189 GeV.

All the visible final states of Z pair decay are investigated. These selections are based on the identification of two fermion pairs, each with a mass close to the Z boson mass, and are different at the two centre-of-mass energies to account for the different signal topology due to the larger boost of the Z bosons at 189 GeV. This boost leads to acollinear and acoplanar fermion pairs. Kinematic fits help in checking the hypothesis of equal mass particles. The $q\bar{q}\nu\bar{\nu}$ and $q\bar{q}q'\bar{q}'$ final states are selected by combining the

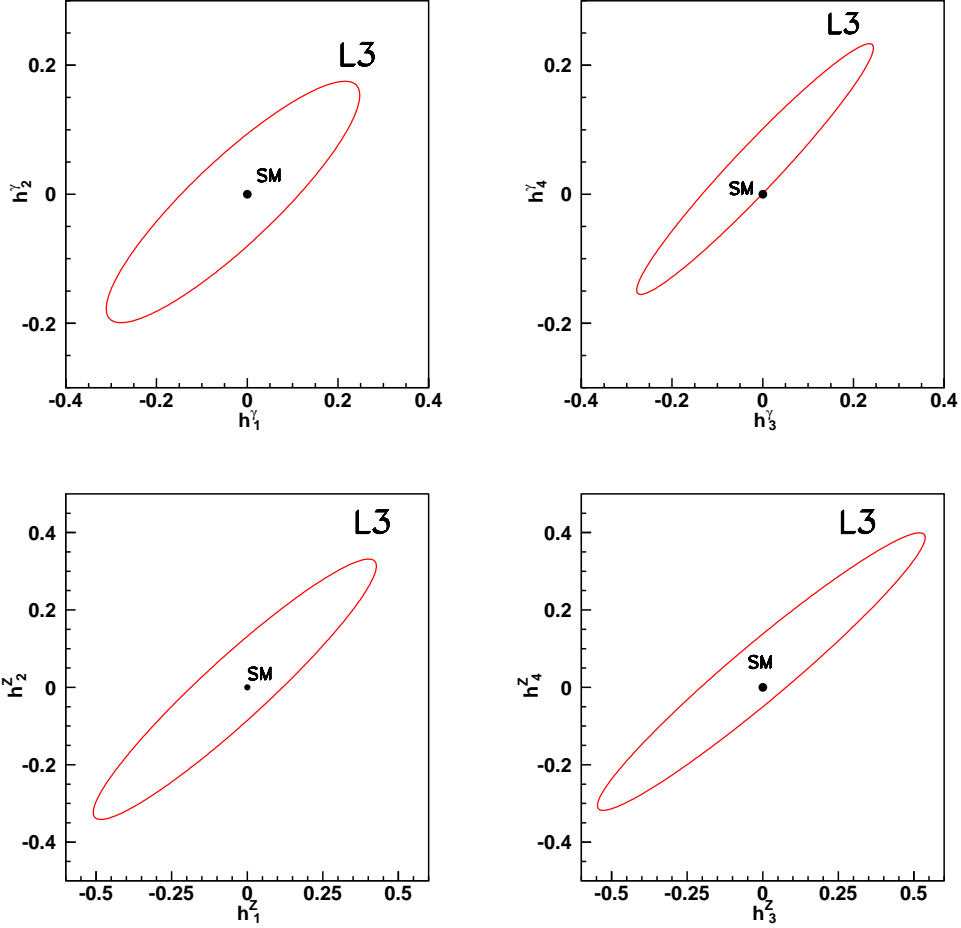


Figure 8: 95% CL contours from simultaneous two-parameter fits to the coupling with the same CP-parity involving the same exchanged vector boson.

kinematic variables into a neural network. Figure 9 presents the reconstructed mass M_{5C} of selected $ZZ \rightarrow q\bar{q}\ell^+\ell^-$ events at 189 GeV after the kinematic fit and the output of the two neural networks for the $q\bar{q}\nu\bar{\nu}$ and $q\bar{q}q'\bar{q}'$ selections.

The ZZ cross sections are determined by a binned maximum likelihood fit to the most discriminating variables of each selection. Within the above mentioned signal definition cuts the results are:

$$\sigma_{e^+e^- \rightarrow ZZ}(183 \text{ GeV}) = 0.30_{-0.16}^{+0.22} {}_{-0.03}^{+0.07} \text{ pb}$$

$$\sigma_{e^+e^- \rightarrow ZZ}(189 \text{ GeV}) = 0.74_{-0.14}^{+0.15} \pm 0.04 \text{ pb},$$

where the first errors are statistical and the second systematic. The first of these values constitutes the first observation of the $e^+e^- \rightarrow ZZ$ process. Figure 10 presents two of the selected data events at $\sqrt{s} = 183 \text{ GeV}$.

It is of particular interest to investigate the rate of ZZ events with b quark content. The production of the minimal or a supersymmetric Higgs boson would give an enhancement of these events and their study on one hand complements the dedicated search for such processes [38, 39] and on the other hand proves the experimental sensitivity to such a signal. The expected Standard Model cross section for the $ZZ \rightarrow b\bar{b}X$ final states at 189 GeV is 0.18 pb.

The investigation of the $ZZ \rightarrow b\bar{b}X$ events proceeds by complementing the analyses of the $q\bar{q}\nu\bar{\nu}$ and $q\bar{q}\ell^+\ell^-$ final states with a further variable describing the b quark content in the event [38, 39], while

the $q\bar{q}q'\bar{q}'$ selection already includes such information to partially reject the W pair background. The combination of these selections yields:

$$\sigma_{ZZ \rightarrow b\bar{b}X}(189 \text{ GeV}) = 0.18^{+0.09}_{-0.07} \pm 0.02 \text{ pb.}$$

The first error is statistical and the second systematic. This result agrees with the SM expectation and differs from zero at 99.9% confidence level. Figure 9 displays these cross sections and their expected evolution with \sqrt{s} .

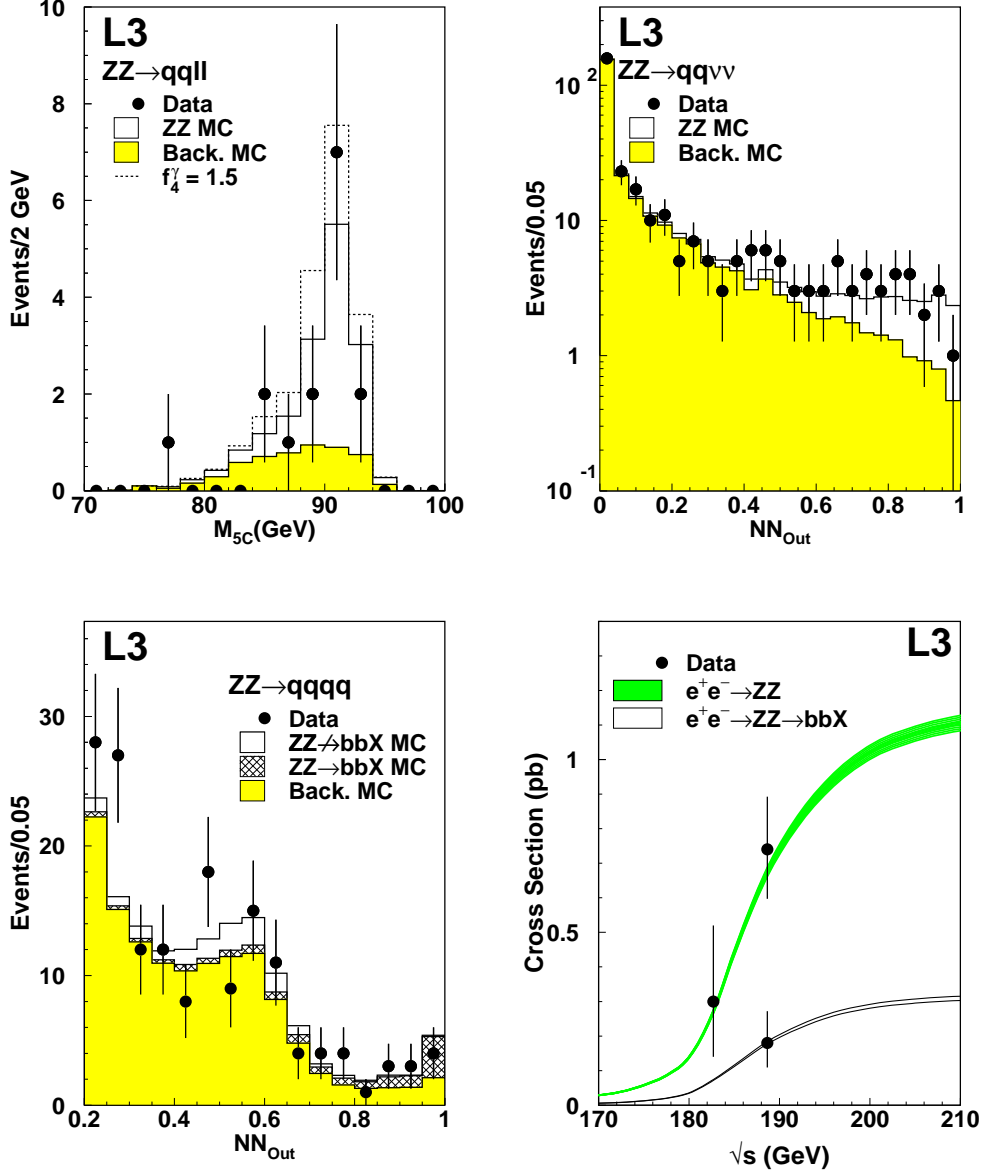


Figure 9: Fit Z mass in $e^+e^- \rightarrow ZZ \rightarrow q\bar{q}\ell^+\ell^-$ events in data and MC together with the distortion expected from anomalous couplings contributions, neural network outputs for the selection of $e^+e^- \rightarrow ZZ \rightarrow q\bar{q}\nu\bar{\nu}$ and $e^+e^- \rightarrow ZZ \rightarrow q\bar{q}q'\bar{q}'$ events and evolution of the $e^+e^- \rightarrow ZZ$ and $e^+e^- \rightarrow ZZ \rightarrow b\bar{b}X$ cross sections with the centre-of-mass energy.

A parametrisation of the ZZZ and $ZZ\gamma$ anomalous couplings is given in References [18, 34]. Assuming on-shell production of a pair of Z bosons, only four couplings f_i^V ($i = 4, 5; V = \gamma, Z$), where the V

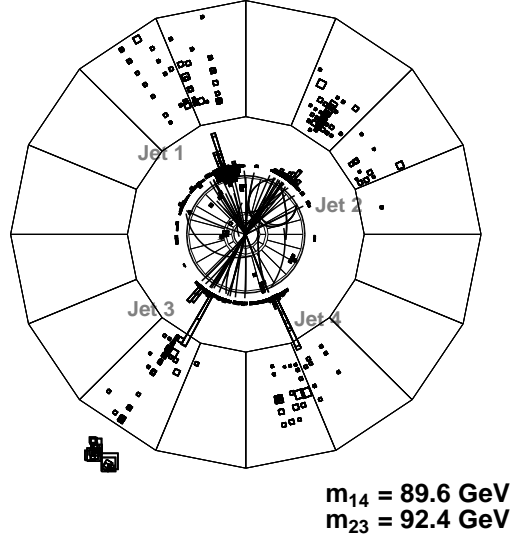
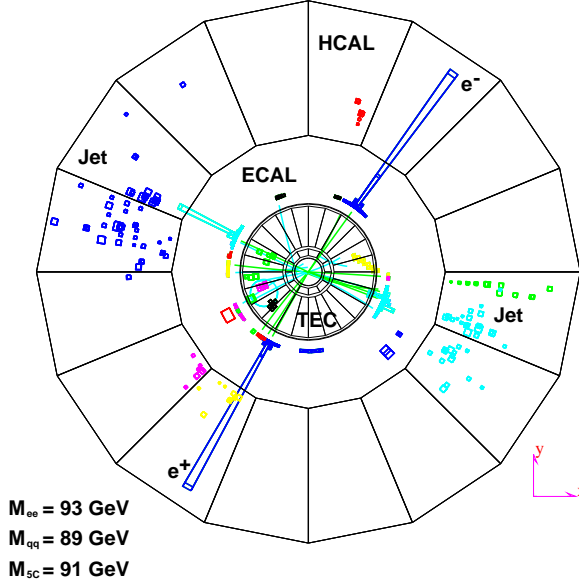


Figure 10: Data events selected by the $e^+e^- \rightarrow ZZ \rightarrow q\bar{q}\ell^+\ell^-$ and $e^+e^- \rightarrow ZZ \rightarrow q\bar{q}q'\bar{q}'$.

superscript corresponds to an anomalous coupling ZZV , may be different from zero. At tree level these couplings are zero in the SM. As in the cases already described above only the real part of these coupling is of interest, if no deviations from the SM are observed. The f_5^V couplings violate the C- and P-symmetries, preserving the CP- one that is instead violated by the f_4^V couplings. These couplings are independent from the h_i^Z ones that parametrise the possible anomalous $ZZ\gamma$ vertex [18, 34], whose investigation was described above.

In order to calculate the impact of anomalous couplings on the measured distributions in the process $e^+e^- \rightarrow f\bar{f}f'\bar{f}'$, the EXCALIBUR generator is extended [40] and used to reweight the SM MC events. Figure 9 displays the effects of an anomalous value of f_4^γ obtained by reweighting with this technique the four-fermion MC events selected by the $q\bar{q}\ell^+\ell^-$ analysis.

The anomalous couplings not only change the ZZ cross section but also the shape of the distributions of several kinematic variables describing the process. A binned maximum likelihood fit is performed on the same discriminating distributions used to determine the cross sections at 183 GeV and 189 GeV. A coupling f_i^V is left free in the fit, fixing the others to zero. The results of these fits are compatible with the SM values and 95% CL limits on the couplings are set as:

$$-1.9 \leq f_4^Z \leq 1.9; \quad -5.0 \leq f_5^Z \leq 4.5; \quad -1.1 \leq f_4^\gamma \leq 1.2; \quad -3.0 \leq f_5^\gamma \leq 2.9.$$

These limits are still valid for off-shell ZZ production where additional couplings are possible. The small asymmetries in these limits are due to the interference term between the anomalous coupling diagram and the Standard Model diagrams.

8 ...in the Extra Dimensions

Several of the results described above are interpreted in the framework of recent theories of the gravitational interaction that introduce extra spatial dimensions. The scene for them is set by two observations. The first is the huge difference between the scales of two of the fundamental interactions of nature, the electroweak ($M_{ew} \sim 10^2 \text{ GeV}$) typical of the SM and the Planck scale ($M_{Pl} \sim 10^{19} \text{ GeV}$) linked to the gravitational constant. The second observation is that collider experiments have successfully tested the SM at its characteristic distance M_{ew}^{-1} while the experimental study of the gravitational force extends only

down to distances of the order of a centimetre [41] thirty three orders of magnitude above the distance M_{Pl}^{-1} .

If n extra spatial dimensions of size R are postulated, the scale of gravity, M_S , may be assumed to be of the same order as M_{ew} explaining the observed difference between M_{ew} and M_{Pl} [42]. In this Low Scale Gravity (LSG) scenario the macroscopic expectations of gravity are preserved by the application of the Gauss' theorem in the extra dimensions:

$$M_{Pl}^2 \sim R^n M_S^{n+2}. \quad (1)$$

The LSG scenario predicts the size R to be just below the unexplored millimetre region, once $n = 2$ and $M_S \sim M_{ew}$. Apart from classical gravitational experiments [41], LSG effects are also accessible via the effects of spin-two gravitons that couple with SM particles and contribute to pair production of bosons and fermions in e^+e^- collisions [43, 44, 45], as described in terms of the parameter M_S [43], interpreted as a cutoff of the theory. It appears as $1/M_S^4$ in the LSG and SM interference terms and as $1/M_S^8$ in the pure graviton exchange process [44, 45]. These terms are multiplied by the factors λ and λ^2 , respectively, which incorporate the dependence on the unknown full LSG theory and are of order unity [43]. To allow for both the possible signs of the interference between the SM and LSG contributions the two cases $\lambda = \pm 1$ are investigated. Figure 11 presents the modification to the $e^+e^- \rightarrow WW \rightarrow q\bar{q}'\ell\nu$, $e^+e^- \rightarrow \gamma\gamma$ and $e^+e^- \rightarrow \mu^+\mu^-$ differential distributions and $e^+e^- \rightarrow e^+e^-$ differential cross sections in presence of LSG.

Process	$M_S(\text{TeV})$	$M_S(\text{TeV})$
	$\lambda = +1$	$\lambda = -1$
$e^+e^- \rightarrow ZZ$	0.77	0.76
$e^+e^- \rightarrow W^+W^-$	0.79	0.68
$e^+e^- \rightarrow \gamma\gamma$	0.79	0.80
Bosons Combined	0.89	0.82
$e^+e^- \rightarrow \mu^+\mu^-$	0.69	0.56
$e^+e^- \rightarrow \tau^+\tau^-$	0.54	0.58
$e^+e^- \rightarrow q\bar{q}$	0.49	0.49
$e^+e^- \rightarrow e^+e^-$	0.98	0.84
Fermions Combined	1.00	0.84
Bosons + Fermions	1.07	0.87

Table 4: Lower limits at 95% CL on the cutoff M_S for different processes and values of λ

From the analysis [46, 47] of the presented distributions as well as hadronic W pair events and τ pairs, together with the discriminating variables of the ZZ event selections and the hadronic cross section, no statistically significant hints for LSG are found in the L3 data at 183 GeV and 189 GeV and the 95% CL limits presented in Table 4 are set on M_S . Assuming that no higher order operators give sizeable contributions to the LSG mediated boson and fermion pair production and that the meaning of the cutoff parameter is the same for all the investigated processes, it is possible to combine the boson and fermion limits. They are as high as 1.07 TeV for $\lambda = +1$ and 0.87 TeV for $\lambda = -1$ at 95% CL and are competitive with those achieved from a combined analysis of the LEP II data [48].

The L3 collaboration also investigated the direct production of a graviton, lost in the extra dimensions, associated with a photon [5, 46] or a Z [47]. The phase space favours the first process. These searches did not yield any evidence for the expected LSG signatures [44, 49] allowing to set 95% CL limits on the LSG scale in excess of 1 TeV.

9 Conclusions and Omissions

This walk through part of the recent L3 results shows a quite wide activity, even on subjects that were not expected to be covered at the start of the LEP II experimental program [25]. On this point all the

experiments match the efforts of the accelerator crew that is impressing the community with record-breaking performance in term of energy, luminosity and operation efficiency.

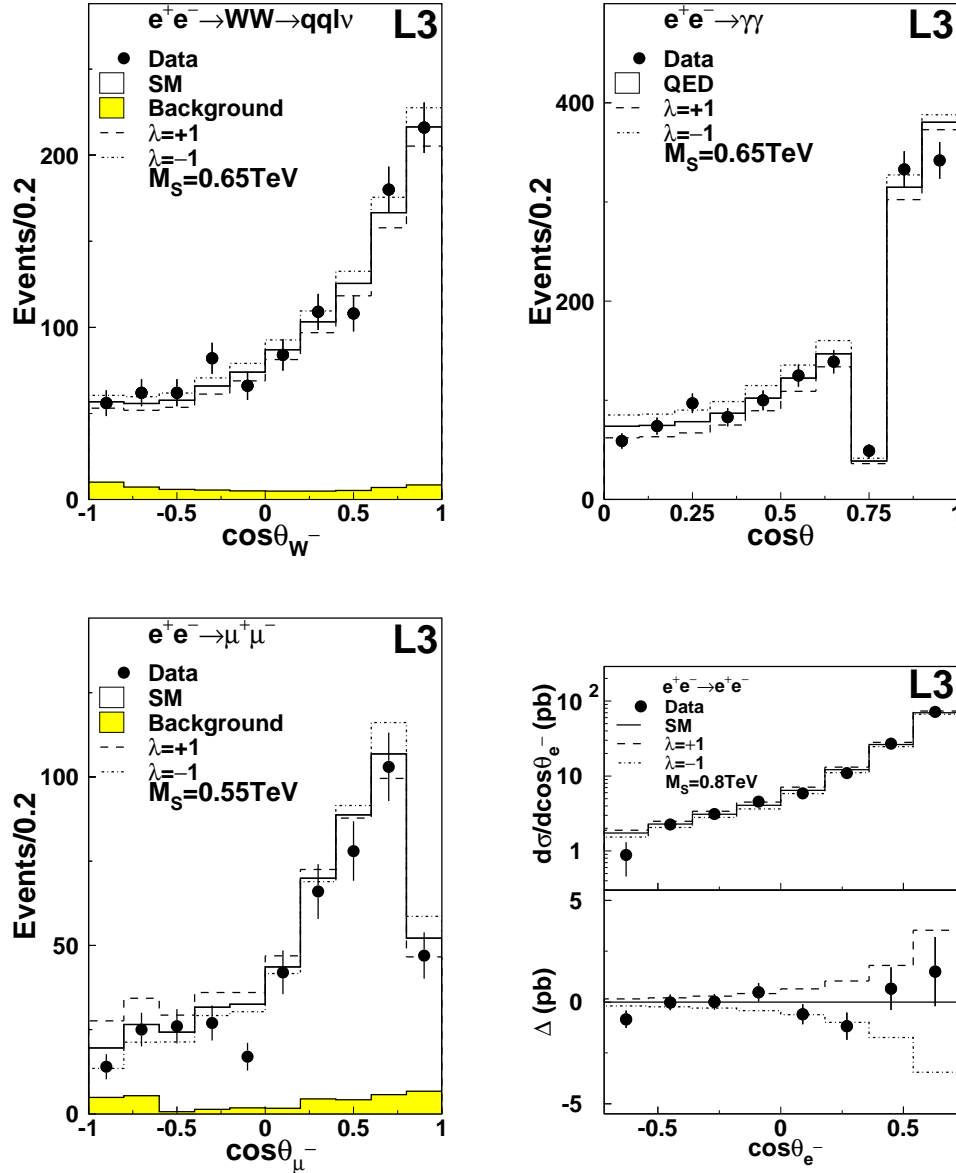


Figure 11: Differential distributions of $e^+e^- \rightarrow WW \rightarrow q\bar{q}'\ell\nu$, $e^+e^- \rightarrow \gamma\gamma$ and $e^+e^- \rightarrow \mu^+\mu^-$ events and differential cross section for the $e^+e^- \rightarrow e^+e^-$ final state. SM expectations and LSG distortions are plotted, for both signs of their interference with SM processes. Data at 189 GeV data are shown.

Several important results have been omitted from this review due to the lack of space and the framework of the discussion. The most important worth mentioning are the 95% CL mass limits on the SM Higgs boson at 95.3 GeV [38] and that on the lightest MSSM neutralino at 32.5 GeV [50], both achieved with the analysis of the full data sample collected by L3 up to 189 GeV. Moreover the L3 experiment has contributed with a large amount of results to the field of two photon physics, as reviewed in Reference [51].

Let me close this review with the hope that something more than precise cross section measurements and interesting limits is awaiting the LEP community in the secrets of the last GeV still to be squeezed from the machine in the high energy runs of 1999 up to a centre-of-mass energy of 202 GeV, and even

beyond, in the final run of the year 2000.

Acknowledgements

I am grateful to my colleagues of the L3 experiment, too numerous to be named here, with whom I shared this challenging physics adventure since I arrived at CERN as an undergraduate student, through the end of the century. It is only with the lively daily interaction with many of them on several of the subjects I described in this work, that I learned something about experimental High Energy Physics.

I wish to thank the organisers of this conference in particular for having helped me to find a swimming pool on the Leninskii prospekt and to fix some complex part of my travel arrangements, two tasks at more than 95% CL beyond the reach of my Russian phrase book.

References

- [1] L3 Collab., B. Adeva *et al.*, Nucl. Inst. Meth. **A 289** (1990) 35; L3 Collab., O. Adriani *et al.*, Physics Reports **236** (1993) 1; M. Chemarin *et al.*, Nucl. Inst. Meth. **A 349** (1994) 345; M. Acciarri *et al.*, Nucl. Inst. Meth. **A 351** (1994) 300; I. C. Brock *et al.*, Nucl. Instr. and Meth. **A 381** (1996) 236; A. Adam *et al.*, Nucl. Inst. Meth. **A 383** (1996) 342; G. Basti *et al.*, Nucl. Inst. Meth. **A 374** (1996) 293;
- [2] S. L. Glashow, Nucl. Phys. **22** (1961) 579; S. Weinberg, Phys. Rev. Lett. **19** (1967) 1264; A. Salam, *Elementary Particle Theory*, pag. 367, Almqvist and Wiksell, Stockholm, 1968.
- [3] J. Mnich, Preprint CERN-EP/99-143, 1999.
- [4] L3 Collab., M. Acciarri *et al.*, contrib. paper #6_262 to the EPS conference, Tampere, Finland 1999.
- [5] L3 Collab., M. Acciarri *et al.*, Preprint hep-ex/9910009, 1999
- [6] L3 Collab., M. Acciarri *et al.*, Phys. Lett. **B 275** (1992) 209; L3 Collab., M. Acciarri *et al.*, Phys. Lett. **B 292** (1992) 463; L3 Collab., M. Acciarri *et al.*, Phys. Lett. **B 431** (1998) 199.
- [7] H. P. Nilles, Phys. Rep. **110** (1984) 1; H. E. Haber and G. L. Kane, Phys. Rep. **117** (1985) 75.
- [8] G. Farrar and P. Fayet, Phys. Lett. **B 76** (1978) 575.
- [9] S. Dimopoulos and L. Hall, Phys. Lett. **B 207** (1987) 210; V. Barger *et al.*, Phys. Rev. **D 40** (1989) 2987.
- [10] L3 Collab., M. Acciarri *et al.*, contrib. paper #6_264 to the EPS conference, Tampere, Finland 1999.
- [11] E. Fermi, Z. Phys. **88** (1934) 161; E. Fermi, Nuovo Cimento **11** (1934) 1.
- [12] E. Eichten *et al.*, Phys. Rev. Lett. **50** (1983) 811.
- [13] L3 Collab., M. Acciarri *et al.*, contrib. paper #6_263 to the EPS conference, Tampere, Finland 1999.
- [14] L3 Collab., M. Acciarri *et al.*, Phys. Lett. **B 370** (1996) 195; L3 Collab., M. Acciarri *et al.*, Phys. Lett. **B 407** (1997) 361.
- [15] A. Van Lysebetten, these Proceedings; R. Tanaka, these Proceedings.
- [16] L3 Collab., M. Acciarri *et al.*, contrib. paper #6_253 to the EPS conference, Tampere, Finland 1999.
- [17] R. Pittau *et al.*, Proceedings of the LEP II Monte Carlo Workshop, to appear as a CERN Report.
- [18] K. Hagiwara *et al.*, Nucl. Phys. **B 282** (1987) 253.
- [19] L3 Collab., M. Acciarri *et al.*, contrib. paper #6_254 to the EPS conference, Tampere, Finland 1999.
- [20] L3 Collab., M. Acciarri *et al.*, contrib. paper #6_255 to the EPS conference, Tampere, Finland 1999.
- [21] L3 Collab., M. Acciarri *et al.*, Phys. Lett. **B 413** (1997) 176;
- [22] L3 Collab., M. Acciarri *et al.*, Phys. Lett. **B 454** (1999) 386;
- [23] L3 Collab., M. Acciarri *et al.*, Phys. Lett. **B 398** (1997) 223;
- [24] L3 Collab., M. Acciarri *et al.*, Phys. Lett. **B 407** (1997) 419;
- [25] *Physics at LEP 2*, Report CERN 96-01 (1996), eds. G. Altarelli, T. Sjöstrand, F. Zwirner.
- [26] L3 Collab., M. Acciarri *et al.*, Phys. Lett. **B 403** (1997) 168.
- [27] L3 Collab., M. Acciarri *et al.*, Phys. Lett. **B 436** (1997) 417; L3 Collab., M. Acciarri *et al.*, contrib. paper #6_256 to the EPS conference, Tampere, Finland 1999.
- [28] R. Kleiss and R. Pittau, Comp. Phys. Comm. **85** (1995) 447.
- [29] J. Fujimoto *et al.*, Comp. Phys. Comm. **100** (1997) 128.

- [30] L3 Collab., M. Acciarri *et al.*, contrib. paper #499 to the ICHEP98 conference, Vancouver, Canada 1998; L3 Collab., M. Acciarri *et al.*, contrib. paper #6_254 to the EPS conference, Tampere, Finland 1999.
- [31] L3 Collab., O. Adriani *et al.*, Phys. Lett. **B 353** (1995) 136; L3 Collab., M. Acciarri *et al.*, Phys. Lett. **B 384** (1996) 323; L3 Collab., M. Acciarri *et al.*, Phys. Lett. **B 413** (1997) 159.
- [32] F. E. Low, Phys. Rev. Lett. **14** (1965) 238; R. P. Feynman, Phys. Rev. **74** (1948) 939; F. M. Renard, Phys. Lett. **B 116** (1982) 264; S. Drell, Ann. Phys. **4** (1958) 75.
- [33] K. Hagiwara *et al.*, Z. Phys. **C 29** (1985) 115; N. Cabibbo *et al.*, Phys. Lett. **B 139** (1984) 459; F. M. Renard, Nucl. Phys. **B 196** (1982) 93.
- [34] G. J. Gounaris *et al.*, Preprint hep-ph/9910395, 1999.
- [35] L3 Collab., M. Acciarri *et al.*, Phys. Lett. **B 436** (1998) 187; L3 Collab., M. Acciarri *et al.*, contrib. paper #6_250 to the EPS conference, Tampere, Finland 1999.
- [36] L3 Collab., M. Acciarri *et al.*, Phys. Lett. **B 450** (1999) 281.
- [37] L3 Collab., M. Acciarri *et al.*, Preprint hep-ex/9909043, 1999.
- [38] L3 Collab., M. Acciarri *et al.*, Phys. Lett. **B 461** (1999) 376.
- [39] L3 Collab., M. Acciarri *et al.*, Preprint hep-ex/9910053, 1999.
- [40] J. Alcaraz *et al.*, Preprint hep-ph/9812435, 1998.
- [41] J. C. Long *et al.*, Nucl. Phys. **B 539** (1999) 23.
- [42] N. Arkani-Hamed *et al.*, Phys. Lett. **B 429** (1998) 263.
- [43] J. Hewett, Phys. Rev. Lett. **82** (1999) 4765.
- [44] G. F. Giudice *et al.*, Nucl. Phys. **B 544** (1999) 3.
- [45] K. Agashe and N. G. Deshpande, Phys. Lett. **B 456** (1999) 60; T. Rizzo, Phys. Rev. **D59** 115010.
- [46] L3 Collab., M. Acciarri *et al.*, Preprint hep-ex/9909019, 1999.
- [47] L3 Collab., M. Acciarri *et al.*, Preprint hep-ex/9910056, 1999.
- [48] S. Mele and E. Sanchez, Preprint hep-ph/9909294, 1999.
- [49] K. Cheung and W.-Y. Keung, Preprint hep-ph/9903294, 1999.
- [50] L3 Collab., M. Acciarri *et al.*, Preprint hep-ex/9910007, 1999.
- [51] M. Wadhwa, Preprint hep-ex/9909001, 1999.